Static friction and arch formation in granular materials

J. Duran, E. Kolb, and L. Vanel
LMDH-URA 800 CNRS, Université Pierre et Marie Curie, 4 place Jussieu, 75252 Paris, France
(Received 12 November 1997; revised manuscript received 13 February 1998)

We report experiments in two and three dimensions that show that the flow mode of a granulate confined in a container strongly depends upon preparation. After a shock or a compressive stress, the granulate can flow freely or exhibit fragmentation resulting from what we call ''vaults hardening.'' We analyze this effect in the framework of a classical triangular bead pattern where the central particle is submitted to a vertical load. The model includes the indetermination of static friction forces and a spring that mimics the elastic tension in a chain of deformable particles. During reversal of gravity, we show that there is a locking mechanism that maximizes the tension of the spring. Then, the magnitude of friction forces is also maximum and may be large enough to prevent any motion of the central particle. This work can be looked upon as an approach to the more general problem of the stability of contact chains in a granulate. [S1063-651X(98)13107-0]

PACS number(s): 81.05.Rm, 46.10.+z, 47.27.Te, 64.75.+g

I. INTRODUCTION

Despite their ubiquity in the surrounding world and their huge industrial interest, granular materials still exhibit numerous unexplained features that have attracted the attention of an increasing number of physicists in the last decade [1]. Among other problems, the frequent occurrence of spontaneous partial or total clogging of ducts and pipes is of crucial importance in industrial processing [2] and still needs to be fundamentally understood. Illustrating the difficulty in tackling this problem from a unified standpoint, numerous experiments and computer simulations have recently been performed. For example, the running hourglass [3,4] stands as an archetype of air (or gas)–particle interactions, which are an important cause of instability for flows in linear pipes [5]. Dynamical simulations of particulate flows quite generally show the occurrence of intermittences [6–8] under various configurations. Granular fragmentation [9–11] may be seen as another facet of the tendency of a granular piling to build up solid inner contact chains that support the overlying material, lean on the side walls of the containers, and are known as vaults or arches. They are responsible for flow discontinuities, which can be observed both in experiments and in computer simulations.

Whatever the processes put forward, the common feature of these observations is a strong local compaction of the piling in certain regions of the space limited by the container walls that results in temporarily or permanently plugging up the flow. Depending on their specific characteristics, the relevant models explain the compaction and plugging as resulting from the formation of dynamic arches [7], from a sort of traffic jam [6], or else from the effect of a dynamic friction that tends to slow down the large blocks of flowing material more than it does the small ones [9]. Yet, all of these models use a simple description of *dynamic* friction interaction, which states that the friction force T, although possibly depending on velocity, is single-valued and is most generally given by an Amonton-Euler equation of the form $T=f_dN$, where f_d is the dynamic friction coefficient and N the normal pressing force.

Leaving aside the dynamic problem, which has recently received some attention, it is tempting to try to get some insight into the static situation. Due to the singularity (or the nonsmooth character [12]) of the friction force at zero velocity, friction can be fully or partially mobilized ($T\leqslant fN$, where f is the static friction coefficient with $f>f_d$), depending on preparation [13] and on the balance of other interacting forces. Henceforth, one may anticipate peculiar plugging or clogging behaviors different from those in the dynamical situation. Industrial reports repeatedly describe evidence of the permanent plugging of huge hoppers containing sand, charcoal, food grains of all sorts, etc. Also, they notice that this permanent plugging quite often occurs after a prolonged period of rest. Then, the granular material seems to be frozen in, refuses to flow when the lower aperture of the hopper is opened, and resists energetic perturbations (such as hammer strokes) before flowing out. This effect may result from some unknown physicochemical interaction between the grains that could occur during the rest period. As we show in the following through a series of laboratory experiments, there is some evidence that permanent plugging occurs even in a supposedly nonreacting and dry material such as silica sand or granular chemical products. These experiments and others do show that permanent plugging depends on preparation. Such a dependence cannot directly arise from the mere extrapolation of the dynamical situation down to zero velocity. Therefore, it turns out that the multivalued character of static friction needs to be accounted for.

The present approach to this problem lies within the limits of our previous observations and models on the problem of progressive fragmentation [9,7], which clearly identified solid vaults to be responsible for dynamic clogging during guided vertical flows of granulates. These vaults or arches were observed to have limited lifetimes. They erratically built up and vanished during the downfall. On the contrary, in the experiments presented here, they may happen with infinite duration and can even resist various moderate perturbations. It is therefore natural to consider that they are more robust than in the dynamic case or, in other words, that there must exist some process that leads to *vault hardening*. It is the major goal of this paper to identify and estimate, at least semiquantitatively, one of the basic processes that may lead

to such a phenomenon. All things considered, it may be looked upon as an attempt to the yet unsolved and more general problem of the stability of granular contact chains.

The second section of this paper is devoted to the description of a few experiments that can be rather easily reproduced under various experimental conditions. Starting either from model or natural materials, they display evidence of long duration or permanent clogging, which depends on the initial preparation. Section III is devoted to introducing some basic considerations about the indetermination of the equilibrium positions and forces in a simple spring-sliding mass toy model. This model serves as an introduction to the analysis of a simplified model involving three spherical particles interacting via static Coulomb friction forces and submitted to a springlike horizontal restoring force (Sec. IV). This basic version of the constitutive element of a granular packing exhibits a sort of *snap-lock effect* that reflects the tendency of the packing under vertical stress to build up hardened vaults by aligning the particles along the direction of the restoring forces. Then, due to the mobilization of static friction forces, the system is seen to retain a memory of the stress history. After removal of the vertical stress, it is left in a more tense situation, which makes it able to resist vertical forces in both upward and downward directions. Section V reports numerical estimates providing support of the model and opens a discussion about the limitations of the proposed analysis. The possibility of computer simulations of vault hardening and permanent plugging effects is mentioned.

II. EXPERIMENTS

One can easily imagine small scale laboratory or table-top experiments able to mimic the permanent plugging effect often encountered in large industrial devices. Here, we describe two typical and simple experiments that exhibit long duration or permanent clogging of a granular flow that would not occur under usual preparative conditions. The first experiment deals with a model granular sample made up of a limited number of particles in reduced two dimensions (Sec. II A). It allows the observation of specific features that, in the present context, help guide the subsequent analysis of permanent clogging. The second experiment concerns a commonly used granular material enclosed in a cylindrical container (Sec. II B). It allows one to get a deeper insight into the subtleties of the influence of the preparation mode and, in particular, to distinguish between isotropic compaction and unidirectional (vertical) stress preparation. A sketch of these experiments is reported in Fig. 1.

A. Particles in two dimensions

We have repeatedly observed permanent plugging in the course of several two-dimensional (2D) experiments performed in flat glass walled cells (typically 15 cm$\times$10 cm; 1.6-mm width) filled with monodisperse 1.5-mm-diam oxidized aluminum beads. Similar devices of various shapes and sizes have been extensively used in our laboratory in order to investigate heaping [14], size segregation [15], and fragmentation during vertical flow [9]. Due to the fact that the cell width is only slightly larger than the bead diameter, these experimental setups have been shown to eliminate the possibility of getting a bead jam across the narrow direction of the cell. In the course of our current experiments, the 2D cell is kept vertically on a stable support and closed with a moving 2D piston (a thin 1-mm-thick metallic blade) that is supported by a cantilever spring pushed vertically by a stepping motor. Although this setup was not specifically designed to generate permanent clogging but rather to analyze the statistics of vaults in a vertically pushed 2D packing, we did observe in several instances that after a set of experiments involving an upward pushing of the 2D pile the piston could be released downwards, resulting in an unexpected feature: The 2D pile did not flow down as expected but would remain compact and suspended in the cell supported by its lowest row of beads, as shown in Fig. 1(1). A careful examination of the situation showed that this feature occurred in the case when all the beads in the lowest row were in contact and also in contact with both lateral walls, thereby forming a vault spanning the space between the two lateral walls. As expected, a slight lateral knock at the front windows would disturb this unstable situation and provoke the free flow of the whole packing.

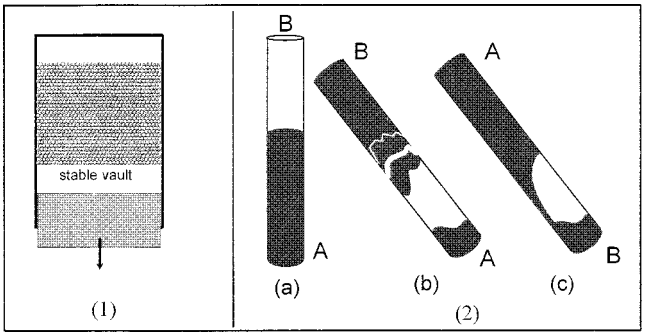

FIG. 1. Two laboratory experiments exhibiting permanent clogging under specific preparation. (1) is a 2D experiment performed in a flat cell while (2) reports a 3D experiment in a cylindrical tube. Each number refers to the description in text.

B. Experiments with sepiolite in a 3D cylindrical container

Sepiolite (hydrated silicate of magnesium $H_4MgSi_3O_{10}$, an equivalent of meerschaum, apparently similar to usual chalk) is a commonly used granular material. Our sample is made of nonspherical millimetric grains, with sizes ranging between 0.2 and 6 mm. A 1-m-long leucite cylindrical tube (inner and outer diameters 65 and 70 mm, respectively) is half full of this granulate. Both ends of the container are fitted with inner plastic caps that are not flush with the tube but slightly recessed with respect to the tips. The sample is initially prepared by gently pouring the granulate into the vertical tube. The lower tip is initially A and we pour the granulate through tip B. As we shall see, the preparation mode turns out to be crucial here so that we have to follow the process carefully.

(i) The subsequent to normal filling of the height reached by the granulate in the tube is h_1 (say, 50 cm). The tube is kept vertical and A is the lowest tip [Fig. 1(2a)].

(ii) Now we turn the tube upside down at an angle far above the repose angle, and, as expected, the granulate flows down continuously along the walls of the tube without showing any fragmentation as sketched in Fig. 1(2c).

(iii) Keeping the tube vertical, we knock the lowest tip (now tip B) of the tube once onto a hard floor. Due to compaction, the height of the granulate in the tube is now slightly reduced by about 1 cm. If now we turn the tube upside down or incline it at an angle far above the repose angle, we observe a completely different flow mode. Then the flow either stops or occurs via a series of successive and ascending fragmentations, as we have previously reported in 2D experiments [9] and as sketched in Fig. 1(2b). Occasionally, the flow stops indefinitely, thereby showing permanent clogging.

(iv) Starting from the same initial situation as in step (iii), we first knock the lowest tip B, but next we knock the upper tip A. The height is reduced by an additional fraction of a centimeter compared to step (iii). We turn the tube upside down: the granulate flows down continuously as in step (ii) and does not exhibit any fragmentation nor permanent clogging.

(v) Starting from the same initial situation as in step (ii) (lowest tip A), we tap repeatedly and energetically over the lateral sides of the tube, thereby inducing a strong compaction of the granulate whose height is now reduced by about 5 cm. If we now invert the tube, the flow occurs continuously as in step (ii).

This series of experiments shows reproducible results. The flow mode depends directly on the tapping sequence and on the tip (lower or upper) at which the tap is applied. By contrast, tapping laterally induces efficient compaction but does not induce clogging. This experiment also works with other commonly used granular materials. Harder materials (such as spherical beads of silica) require a more energetic sequence of taps (possibly with a hammer) in order to allow the observation of similar behavior.

These experiments and some others (e.g., see the influence of the pouring mode in filling containers [17]) not only exhibit the crucial importance of the preparation mode but also attract attention to the preparation anisotropy in the balance of forces in the granulate. This anisotropy and the fact that similar experimental observations can be made in 2D or 3D with spherical beads allow one to rule out the possibility that the observed effects are merely due to the formation of geometric arches, which could be obtained with angular particles. In particular, the sepiolite experiments indicate that, at least under these circumstances, compaction [18–24] is not merely and directly correlated to subsequent flow behavior and to clogging probability.

As we show in the following, the consideration of mobilization of static friction forces in the course of preparation is able to render most (if not all) of the observed effects. Before attempting to build up a specific model for granulates and in order to introduce the problem, we now examine a simple toy model, which helps us to understand the basic mechanism that can explain how a contact chain in a granulate can keep the memory of the preceding history.

III. TOY MODEL AND MECHANICAL HYSTERESIS

We first examine the experimental setup sketched in Fig. 2(a). It consists of a rough block (mass m) resting on a rough inclined plane and attached from below to a spring. The plane can be rotated around its lowest side from $\theta=0$ to $\pi/2$. An elementary experiment consists in starting with the plane standing at a vertical position and *slowly* tilting the angle θ down to zero and back from 0 to $\pi/2$. As expected, experiments show that the mass m will gradually go down and climb up along the board as the angle θ is increased or decreased. Let $x(\theta)$ be the elongation of the spring [which means that $x(\theta)\equiv 0$ at rest, i.e., if $m=0$]. If there were no block-plane friction involved, $x(\theta)$ would be a continuous monotonic function $x(\theta)\propto \sin\theta$ [central dotted line in Fig. 2(b)]. Instead, when a significant block-plane friction is involved, we observe that when increasing (decreasing) the angle θ, the block position follows a staircaselike process, as pictured (full lines) in Fig. 2(b).

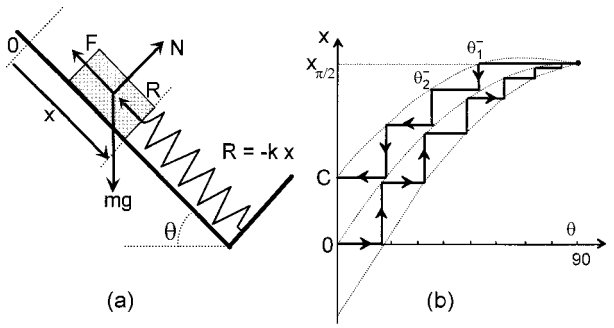

FIG. 2. Spring-mass model displaying position indetermination due to static friction. (a) is a diagram of the balance of forces when the board is progressively tilted from horizontal to vertical when the friction force acts upwards. (b) schematically displays the spring deformation as a function of the angle θ. The origin of the coordinates is chosen at the equilibrium point of the spring without any load. The process shown starts from its maximum value when the board is vertical and the elongation decreases to C when the board is horizontal. $C=mgf/k$. The upper (lower) dotted line corresponds to the limiting curve $\varepsilon=+1$ ($\varepsilon=-1$).

The weight mg (g is the acceleration of gravity) is balanced in the normal direction by the reaction $N=mg\cos\theta$ and in the tangential direction by the frictional resistance to motion F and the force R due to the spring compression. According to Amonton's friction law, the normal N component results in generating a tangential force opposing relative motion, which reads $F=\varepsilon fmg\cos\theta$, where ε is a dimensionless parameter that may take any value between $+1$ and -1 and whose actual value is determined by the history of the process. In the following, we will consider for the sake of simplicity that the coefficient of dynamic friction is null.

Starting from a vertical position where the spring compression is maximum ($x_{\pi/2}=mg/k$, where k is the spring force constant), we decrease progressively and slowly the angle θ down to zero (thereby noting θ^-). At the very beginning of the process, the friction force $mg\varepsilon f\cos\theta$ comes into play and prevents the mass from sliding upwards until ε reaches its maximum value $\varepsilon=1$, which determines the beginning of the sliding process. As long as $\varepsilon<1$, the elongation remains equal to $x_{\pi/2}$. The position for which $\varepsilon=1$ (when the angle is different from $\pi/2$) is determined by the solution of the equation for the force balance in the x direction with no net force:

$$\frac{k}{mg}x_{\pi/2}=1=\sin\theta_1^-+f\cos\theta_1^-. \qquad (1)$$

Then the mass slides upwards. In case of a null dynamic friction coefficient, the block would be subjected to the natural oscillation of a free spring-mass system. For the sake of simplification, we consider here that the spring motion is efficiently damped (e.g., with an additional dashpot), so that the spring elongation approaches exponentially the point $x_{\theta_1^-}=(mg/k)\sin\theta_1^-$ $(\varepsilon=0)$. The process goes on through a succession of plateaus and ascents that are obtained by a similar recursive procedure and that are defined by the angle θ_i^-, which obeys the equation $\sin\theta_i^-=(\sin\theta_{i+1}^-+f\cos\theta_{i+1}^-)$. As every step is linked to the preceding one, we see that all successive positions depend on the previous position. In brief, the spring elongation retains a memory of the previous mass position, at every step.

Performing a reverse sequence, i.e., starting from a situation when $\theta=0$, we are faced with the definition of the initial position. The mass can be initially set at any position x_i satisfying the equation $kx_i=mg\varepsilon f$ with $\varepsilon\in[-1,+1]$. When θ is increased the subsequent trajectory again shows plateaus and up-motions in the (x,θ) space determined by oscillations of ε between 0 and -1. Under these circumstances, the reverse trajectory in the (x,θ) space separates from the preceding one and lies below the descent trajectory, as reported in Fig. 2(b). The recursive procedure leads to successive positions obtained at angle θ_i^+ obeying $\sin\theta_i^+=(\sin\theta_{i+1}^+ -f\cos\theta_{i+1}^+)$. In short, the mass can be initially set at any position lying in the region delimited by the curves $(k/mg)x=\sin\theta\pm f\cos\theta$ in the $x(\theta)$ diagram [dotted lines in Fig. 2(b)]. Starting from a particular situation determines definitely the subsequent process. Rather than numerically solving the equations, the set of stable positions can be easily obtained by drawing the staircase picture on the $x(\theta)$ diagram, as shown in Fig. 2(b).

Thus, as the angle θ is successively increased and decreased, the mass follows a staircaselike motion limited by a hysteresis cycle whose area reflects the irreversibility due to friction dissipation during the process. This observation is not novel in itself. It is related both to the well known stick-slip process in spring-mass models and to Mindlin and Deresiewicz's investigation of the loading and unloading hysteresis cycles of elastic spheres in contact [13].

It will become apparent that the hysteretic behavior of the spring-mass system may be relevant to the understanding of the experiments described in Sec. II. As we will see in more detail in Sec. IV B, it can be intuitively understood that the elastic deformation of contact chains in a granulate can play the role of the spring in the preceding toy model.

IV. FRICTION HYSTERESIS OF SPHERES IN CONTACT IN A GRANULAR PACKING

A. Model

We turn back to the problem of a dense bead packing made up of a large number of spherical particles confined by gravity to a vertical cylindrical container. We recall that when the container is turned upside down, the state of stress may be such that the granular material will resist the pulling effect of gravity, and a transient or permanent vault structure will be observed. Clearly, if we admit that the friction forces are responsible for the vault effect, the possibility for a vault to exist will depend on how the friction forces have been mobilized before turning the container upside down. In other words, when gravity is reversed, the friction forces must be in the opposite direction to gravity and large enough. In the following, we present a heuristic model that captures some of the features observed in the experiments. In the process of gravity reversal, the model exhibits either a ''vault hardening'' or a ''vault softening'' behavior. Each of these behaviors provides a very simple mechanism for the explanation of the fragmented flowing mode or the continuous flowing mode. The selection of a specific behavior is mainly dependent on the stress history as the flowing mode in the experiments.

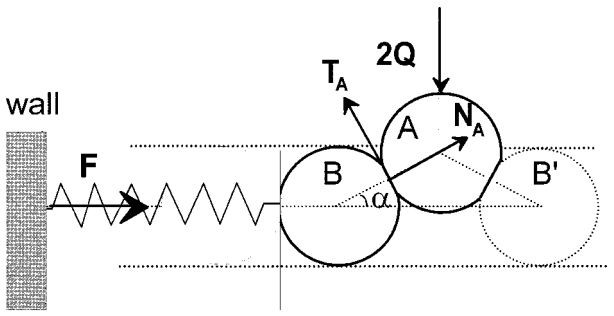

FIG. 3. Balance of forces in the triangular basic pattern (see text). Bead A moves vertically while all other beads are moving along a horizontal line. The weight of the beads and the vertical components of the forces are balanced by the reaction of a horizontal channel depicted by the dotted lines.

Let us consider a horizontal chain of spherical particles squeezed between two rigid lateral walls. The particles lie on a floor and are forced to move horizontally as if they were guided in a channel. The particles are deformable and there are no frictional interactions among them. We suppose that the total deformation of the chain can be large enough for an additional particle A to be inserted. In a real situation, bead A would tend to dislodge a neighboring bead from the chain, but it is not the purpose of the model to study such an instability. Particle A is supposed to have frictional contacts with beads B and B′ (see Fig. 3) and the friction forces can take any values in Coulomb's cone of friction. The elastic response of the remaining particles is represented by a spring between bead B (B′) and the lateral wall. For the sake of simplicity, we suppose that bead A is moving vertically and that beads B and B′ have symmetrical behaviors. We call α the penetration angle, which is explicitly defined in Fig. 3. The variation of the angle α is mainly due to the elongation of the lateral springs, and the contribution of the deformations of beads A, B, and B′ is neglected; bead A is subject to a vertical and downward (positive) force $2Q$, which includes both the applied load on bead A and its own weight. The load applied to bead A is varied slowly in a quasistatic way, such that, at any time, static equilibrium is realized for the whole system. As long as the friction forces have not reached the Coulomb limit for sliding, bead A remains at rest, but the friction forces evolve so as to balance the variation of the load on bead A. When the friction forces reach the sliding limit, bead A can slide on beads B and B′ and move down (or up) while keeping load Q constant, until it reaches an equilibrium for which no friction forces are mobilized as in the preceding toy model. Bead B is subject to a positive (i.e.,

from left to right) and horizontal compressive force F from the spring, which is only a geometrical function. Bead B is also subject to its own weight W and to a normal reaction force R, which prevents vertical motion either in the upward or downward direction. In a real situation, significant vertical motion would be limited by the surrounding granular material. In the contact area with bead B (B′), bead A is submitted to a normal load N_A (N'_A) and a tangential load T_A (T'_A), while bead B (B′) is subjected to a normal load $-N_A$ ($-N'_A$) and a tangential load $-T_A$ ($-T'_A$). The symmetry of the problem implies that $N_A=N'_A$ and $T_A=T'_A$. Then, the equilibrium of bead A reads

along the *horizontal* axis:

$$N_A \cos\alpha - T_A \sin\alpha - N'_A \cos\alpha + T'_A \sin\alpha = 0, \quad (2)$$

along the *vertical* axis:

$$T_A \cos\alpha + N_A \sin\alpha + T'_A \cos\alpha + N'_A \sin\alpha = 2Q. \quad (3)$$

Given the symmetry relations, the equilibrium is always satisfied along the *horizontal* axis and the equilibrium along the vertical axis is reduced to

$$T_A \cos\alpha + N_A \sin\alpha = Q. \quad (4)$$

Similarly, the equilibrium of bead B reads

along the *horizontal* axis: $$-T_A \sin\alpha + N_A \cos\alpha = F, \quad (5)$$

along the *vertical* axis:

$$R - W - T_A \cos\alpha - N_A \sin\alpha = 0. \quad (6)$$

The equilibrium along the vertical axis can always be satisfied by a suitable choice of reaction force R. Thus, the equilibrium of bead B simply requires that

$$-T_A \sin\alpha + N_A \cos\alpha = F. \quad (7)$$

Then, it is straightforward to find the following:

$$N_A = Q \sin\alpha + F \cos\alpha,$$

$$T_A = Q \cos\alpha - F \sin\alpha. \quad (8)$$

We introduce the friction condition, as in the preceding section. It reads

$$T_A = \varepsilon f N_A, \quad \varepsilon \in [-1,+1], \quad (9)$$

where f is the coefficient of static friction. Eventually, it gives a relationship between F and Q for a particular mobilization of the friction forces (ε value):

$$F = Q \frac{1-\varepsilon f \tan\alpha}{\tan\alpha + \varepsilon f}. \quad (10)$$

At a given α, and depending upon the loading or unloading sequence, ε ranges between $[0,+1]$ (loading sequence) and $[0,-1]$ (unloading sequence). When the friction balances and adjusts to the variation of the applied force (i.e., when $|\varepsilon|<1$), α is expected to remain constant. The angle α relaxes (increases or decreases) when the condition $\varepsilon=\pm 1$ is reached and we have to solve the no-friction problem ($\varepsilon=0$) for a fixed load Q. Under this slip condition, Eq. (10) reduces to $F=Q\cot\alpha$. Another relationship between α and F has to be found in order to determine the equilibrium state. This relationship depends on the elasticity model for the granulate contact chains. Obviously and provided no global reorganization of the relative positions of the particles occurs under loading or unloading, F is expected to be a monotonically decreasing function of α.

We do not know the detailed function $F(\alpha)$, which is largely dependent on the microscopic details of the bead-bead interface and on the elasticity model considered for the contact interactions. Being monotonic, $F(\alpha)$ spans the range $F_{\min}$ to $F_{\max}$ when α decreases from $\pi/3$ down to 0. This function is expected to scale differently according to the model used for the description of the contact interaction. If we denote $u(\alpha)$ the longitudinal chain deformation, the scaling exponent β of the elastic force $F\propto[u(\alpha)]^\beta$ is 1 for a linear model, 3/2 for the classical Hertz model, and 2 for a ''soft crust'' or multicontact model [25]. Then F reads

$$F=[2(1-\cos\alpha)F_{\min}^{1/\beta}+(2\cos\alpha-1)F_{\max}^{1/\beta}]^\beta \quad \text{with} \quad \beta=1,3/2,2, \quad (11)$$

whence, inserting expression (11) into Eq. (10) provides the $Q(\alpha)$ dependence:

$$Q=[2(1-\cos\alpha)F_{\min}^{1/\beta}+(2\cos\alpha-1)F_{\max}^{1/\beta}]^\beta \frac{\tan\alpha+\varepsilon f}{1-\varepsilon f\tan\alpha} \quad \text{with} \quad \varepsilon\in[-1,+1]. \quad (12)$$

For the sake of illustration, we consider here the case of a linear spring model ($\beta=1$) and take $F_{\min}$ vanishingly small. More sophisticated models for the contact interaction can be considered. However, provided that the basic assumption of the monotonicity of the $F(\alpha)$ is preserved, the results will not separate, at least qualitatively, from the simple linear case. Then Eq. (12) reduces to

$$Q=F_{\max}(2\cos\alpha-1)\frac{\tan\alpha+\varepsilon f}{1-\varepsilon f\tan\alpha}. \quad (13)$$

The graph of this equation is given in Fig. 4.

The particular shape of the α dependence of Q requires some analysis. Using the same description as in Sec. III, we observe that the static friction condition implies that the representative point of the equilibrium has to lie in the region delimited by the $\varepsilon=+1$ and $\varepsilon=-1$ curves, respectively, above and below the no-friction curve corresponding to $\varepsilon=0$. This means that, at a given angle α, loading bead A (i.e., increasing the load Q) over the point noted L will result in an abrupt relaxation of the system. The same feature occurs symmetrically if we reduce the load below the point marked U (unload) in the diagram. As we have seen previously, the actual stable position of the representative point at a given angle α lies on the UL segment and depends on the preparation.

The ridged shaped $Q(\alpha)$ curve in Fig. 4 has a direct consequence that is relevant to the generic problem of the sta-

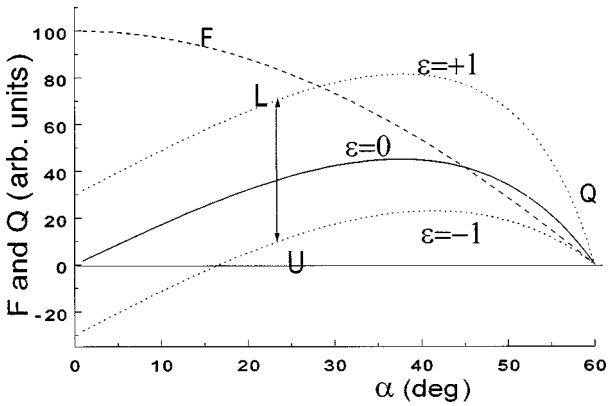

FIG. 4. Q and F dependence on the penetration angle α in the linear spring model. Here $F_{\min}=0$, $F_{\max}=100$ arb. units, and $f=0.3$. The set of the three curves $Q(\alpha)$ are obtained for $\varepsilon=0$ (central full line) and $\varepsilon=\pm 1$ (dashed lines). L and U stand for ''load'' and ''unload,'' respectively (see text). Forces are expressed in arbitrary units.

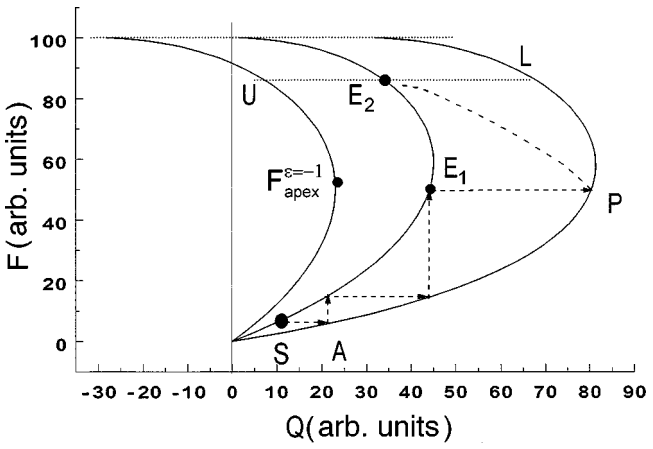

FIG. 5. Representation of the behavior of the system in the $F(Q)$ space. Here $F_{\min}=0$, $F_{\max}=100$ arb. units, and $f=0.3$. The staircaselike dashed line shows a typical trajectory (see text). The three solid curves represent $\varepsilon=1,0,-1$. Forces are expressed in arbitrary units.

bility of vaults in a granulate. We first analyze the situation when there is no friction ($\varepsilon=0$). In the whole range $[0,\pi/3]$, a decrease of α results in an increase of F, which reads $\partial_\alpha F<0$. In contrast, independent of the model for the chain deformation (i.e., if $\beta=1, 3/2,$ *or* 2), the function $Q(\alpha)$ is not monotonic and happens to exhibit two distinct domains where $\partial_\alpha Q$ is positive, null, or negative. The region where $\partial_\alpha Q$ is negative corresponds to a domain where the spring drawback force F increases when the load Q is increased. This results in a positive reaction, which tends to restore the initial angle α when the system is unloaded. On the contrary, going into the domain where $\partial_\alpha Q$ is positive corresponds to triggering a sort of ''snap-lock effect.'' If the stress Q is increased above the maximum in the curve $\varepsilon=0$ (full line) of Fig. 4, the system becomes unstable, since the load Q is larger than any equilibrium value. Then, the beads tend to align down to $\alpha=0$ instead of restoring the initial α starting value, and the spring drawback force F tends towards its maximum value. As we see in the following, a combination of this snap-lock effect and the mobilization of friction forces may explain several unusual behaviors, such as vault hardening, as observed in Sec. II.

Now we turn back to the question of the mobilization of friction forces in the spirit of the spring-mass model examined in Sec. III. We look for the detailed trajectories of the system in the $F(Q)$ space that is the analog to the $x(\theta)$ representation (see Fig. 3). The graph of this function is given in Fig. 5.

Starting from a given position (S in the figure), i.e., from a given F and Q at a definite penetration angle α ($\varepsilon=0$), and increasing progressively Q, we can calculate analytically the successive positions of the system using the same arguments as in Sec. III. Rather than performing the complete calculation, it turns out to be much more convenient to use the diagrammatic representation pictured in Fig. 5. In the region where $\partial_Q F$ is positive, the trajectory follows a series of stick-slip events such as those in the simple spring-mass model. This occurs until the point P is reached. At this point, a slightly increasing force Q will break the friction force and trigger the snap-lock effect. The spring drawback force F cannot balance the opposite resultant force on bead B due to the applied load Q anymore, and this results in an abrupt decrease of the penetration angle α down to some point marked E_2 in the figure. The process leading from point P to point E_2 is an out-of-equilibrium process during which the initially fixed force Q must decrease in order for the system to reach a new equilibrium state. The complete determination of this equilibrium state depends on the time dependence of the Q force, and could be performed by analytically solving the full mechanical problem. In view of the crude approximations of the present model (and in particular of the simplification by which the dynamical friction coefficient is zero), we restrict this discussion to a semiquantitative description and will not delve any further into the details of the model.

Figure 5 provides a visual support of the terms ''vault hardening'' and ''vault softening'' that we already used earlier in this paper. To simulate the reversal of gravity, the load Q is now slowly decreased and we search for stable positions for which Q becomes negative. Whenever the system is in a situation for which $F<F_{\text{apex}}^{\varepsilon=-1}$ (for example, point E_1), a decrease in load Q will lead to a decrease in the compressive force F until it reaches $F=0$ when $Q=0$ after successive stick-slip events. Afterwards, if Q becomes negative, there will be no friction forces to prevent bead A from losing contact with beads B and B′. This is what we call ''*vault softening*'' and corresponds to the continuous flowing mode in the experiments. On the contrary, whenever the system is in a situation when $F>F_{\text{apex}}^{\varepsilon=-1}$ (for example, point E_2), a decrease in load Q will lead to an increase in the compressive force F, and negative values of Q will eventually be reached after successive stick-slip events. The maximum negative value $Q_{\max}=-fF_{\max}$ is reached when $\alpha=0$ and $\varepsilon=-1$, i.e., when the compressive force F is maximum. If ever $Q_{\max}$ is large enough, bead A will be able to resist the pulling effect of gravity. This is what we call ''*vault hardening*'' and corresponds to a permanent clogging or a fragmented flowing mode in the experiments.

The model can be related to the series of experiments reported in Sec. II as follows. Starting from usual preparative

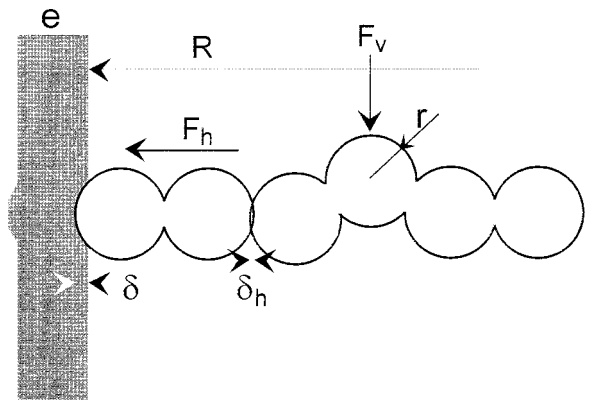

FIG. 6. Definition of the parameters for calculating the overall deformation of the linear chain of contacts.

conditions, the granulates flow normally when the container is turned upside down. After a static compression or a sequence of compressive shocks in one specific direction, several contact chains in the granular material, which are able to resist the pulling forces due to the reversal of gravitational forces, are left in a more tense situation. Inversely, shocks in the opposite direction [Sec. II B, step (iv)] tend to relax the tension of the vaults thereby allowing a free flow mode.

B. Spring and drawback force: Numerical estimate

In the preceding section, we have shown that a simple spring-rubbing mass model is, in principle, able to render several basic features of vault hardening. This model establishes a relationship between the geometry of a triangular pattern (through dependence on α) and the mobilization of friction forces. It implies a significant relative motion of the beads in the packing. A simple order of magnitude calculation helps to show that this may occur under usual experimental conditions. In the following, we successively consider semiquantitatively the deformation of a linear chain of contacts and the consequence of the deformations of the container walls within the context of the Hertz model.

Consider a vertical cylindrical container (radius R, see Fig. 6) made up of a material whose Young's modulus is E'. The wall thickness is $e \ll R$. The container is filled with a large number of spherical beads (radius $r \ll R$, Young's modulus $E \gg E'$). Let g be the gravitational acceleration and suppose that a vertical fast motion (such as a shock) is able to temporarily change the effective force by a positive or negative adimensional factor Γ.

Depending upon experimental conditions, $|\Gamma|$ ranges between 1 and 10. We consider a typical contact chain of $n \sim R/r$ particles that spans the space between both lateral walls in the container. Let F_v be the typical vertical force due to gravity, supported by a bead in the packing. Basic Janssen arguments [16] indicate that a bead situated in the bulk of the packing undergoes a maximum vertical stress that is typically equivalent to the weight of $2n$ beads. If ρ is the specific mass of the beads, we have $F_v = n\Gamma\rho g \frac{8}{3}\pi r^3$. Again using Janssen's arguments [17], we know that about a fraction $K = 30\%$ of the vertical stress is converted into a horizontal one directed towards the lateral walls. This results in a horizontal force on a bead F_h, such that $F_h = nK\Gamma\rho g \frac{8}{3}\pi r^3$. If δ_h is the penetration of two beads in contact, one easily finds that the retraction of a typical contact chain due to internal pressure in a granulate is $\Delta = n\delta_h \propto n(F_h^2/E^2 r)^{1/3} \propto \Gamma^{2/3} R^{5/3}$, which does not depend on the particle size. Using typical numerical values (i.e., $\rho = 2000$ kg/m^3, $R = 0.1$ m, and $E = 10^{10}$ N/m^2), one finds that at $\Gamma = 1$ (which means under its own weight), $n\delta_h$ is of order 10 μm which can be increased up to about 50 μm under a shock at $10g$. Using softer materials for the beads such as leucite or, even more, sepiolite, allows us to cover a deformation range up to 100 μm which means a significant fraction of a typical bead diameter. Note that this deformation is large enough to trigger the *snap-lock effect* under a moderate external perturbation, particularly if the force along the contact chain is close to F_{apex}.

In some typical experimental situations, the container walls are likely to undergo a much larger deformation than the beads' chain. These wall deformations can also render the effect of the spring deformation. The following simple calculation can be performed. Suppose we consider a leucite tube whose Young's modulus is E'. Suppose that the tube is entirely filled with a granular material. In a layer of thickness $2r$, there are typically $N = \pi n$ beads in contact with the wall and each bead applies a compressive force F_h. The cumulative effects of these compressive forces create an equivalent pressure on the internal wall of the cylinder whose maximum value can be written as $p \simeq NF_h/2\pi Rb$, b being the diameter of the contact circle at the bead-wall interface. The general solution for the stress distribution in a hollow cylinder with uniform internal and external pressures is a classical problem [26] that is easily solved in polar coordinates (r, θ). If there is no pressure applied on the external wall, and in the approximation of small thickness $e \ll R$, the general solution reduces to a uniform tensile stress $\sigma_\theta \simeq pR/e$, a tangential strain $\varepsilon_\theta \simeq \sigma_\theta/E'$, and a radial displacement $\delta_r = R\varepsilon_\theta$,

$$\delta_r \simeq \frac{F_h}{E'b}\frac{NR}{2\pi e} \simeq \frac{\delta_h}{2}\frac{E}{E'}\frac{R^2}{2\pi r e} \simeq n\delta_h \frac{E}{4E'}\frac{R}{e} \simeq \Delta \frac{E}{4E'}\frac{R}{e}.$$

In a typical example corresponding to the 3D experiment described in Sec. II B, $R = 0.1$ m, $e = 1$ mm, $E' = E/4$, thus $\Delta \simeq 10$ μm, and even more if there is a shock, so that typically $\delta_r \simeq 1$ mm. It means that the deformation of the container walls can be several tens of times larger than the deformation of the contact chains. When subjected to an energetic shock, the wall deformation can be as large as several hundreds of micrometers (which can mean on the order of several particle sizes for powders or fine granular materials). In large industrial vessels such as hoppers or tubes with thin walls, the wall deformation can significantly contribute to vaults hardening, as investigated in the present paper.

V. DISCUSSION AND CONCLUSION

The present work shows that permanent plugging, which is frequently observed in industrial situations, can be readily obtained in small scale laboratory experiments using an adequate preparation of the granular material that otherwise would flow continuously. Starting from a few simple experiments and basic arguments, we attract attention to the crucial importance of the interplay of the geometry and mobilization

of friction forces in determining the stress equilibrium of a granulate confined in a container.

Our model takes advantage of a detailed analysis of the balance of forces, which includes friction mobilization and reaction to compressive stresses in an elementary three-bead model. It is seen that, under particular circumstances, the granular system can build up tense inner contact chains that are able to resist moderate perturbations. In turn, these hardened vaults can oppose further internal motion, leading to permanent plugging or to fragmentation.

Besides using the classical Amonton static friction law, this model is based on the hypothesis that the granular system resists horizontal compression by mobilizing an elastic restoring force whose intensity depends monotonically on the compression. This is certainly a crude approximation in the case of plastic deformation that is likely to occur in many chemical or food grain materials. There, the snap-lock effect may occur via plasticity or via a creeping process. Note that under these circumstances and at the apex of the curve in Fig. 5, a slow creep is able to induce an abrupt relaxation of the grain positions, leading to a consolidation of the contact chains. Within this context, we may speculate that this effect would be at the origin of the vault hardening and permanent clogging observed in many industrial hoppers after a prolonged period of rest.

Our model, which deals with a three-bead pattern, oversimplifies the description of the complex network of forces in a granulate, as depicted for example in [24]. The question arises whether a correct computer simulation of these static or quasistatic effects that originate from the basic static indetermination of the friction forces is possible. At present, most computer simulations in the physics of granular materials make use of a dynamic description of the shock and friction interactions. Quite generally, the algorithms are implemented with a single-valued friction coefficient, and a permanent relative motion of the particles is required in order to solve dynamical equations. The question arises of how to know whether a full implementation of the static contact interaction (such as in [27]) is able to render a correct description of the vault hardening effect.

ACKNOWLEDGMENTS

This paper has benefited from the support of the French Groupement de Recherche sur la Physique de la Matière Hétérogène et Complexe (CNRS) and of the corresponding HCM European network. Fruitful discussions with P-G. de Gennes, J. Goddard, and J-C. Charmet are acknowledged.

[1] H. M. Jaeger, S. R. Nagel, and R. P. Behringer. Rev. Mod. Phys. **68**, 1259 (1996).
[2] B. J. Ennis, J. Green, and R. Davis, Chem. Eng. Prog. **90**, 32 (1994).
[3] T. Le Pennec, K. J. Måloy, A. Hansen, M. Ammi, D. Bideau, and X. L. Wu, Phys. Rev. E **53**, 2257 (1996).
[4] G. H. Ristow and H. J. Herrmann, Physica A **213**, 474 (1995).
[5] T. Raafat, J. P. Hulin, and H. J. Herrmann, Phys. Rev. E **53**, 4345 (1996).
[6] D. C. Hong, S. Yue, J. K. Rudra, M. Y. Choi, and Y. W. Kim, Mod. Phys. Lett. B **6**, 761 (1992).
[7] S. Luding, J. Duran, T. Mazozi, E. Clément, and J. Rajchenbach, *Simulations of Granular Flow: Cracks in a Falling Sandpile* (World Scientific, Singapore, 1996).
[8] G. Peng and H. J. Herrmann, Phys. Rev. E **49**, 1796 (1994).
[9] J. Duran, T. Mazozi, S. Luding, E. Clément, and J. Rajchenbach, Phys. Rev. E **53**, 1923 (1996).
[10] S. Luding, J. Duran, E. Clément, and J. Rajchenbach, J. Phys. I **6**, 823 (1996).
[11] J. Duran, *Sables, Poudres et Grains* (Eyrolles, Paris, 1997).
[12] F. Radjai, L. Brendel, and S. Roux, Phys. Rev. E **54**, 861 (1996).
[13] R. D. Mindlin and H. Deresiewicz, J. Appl. Mech. **20**, 327 (1953).
[14] E. Clément, J. Duran, and J. Rajchenbach, Phys. Rev. Lett. **69**, 1189 (1992).
[15] J. Duran, T. Mazozi, E. Clément, and J. Rajchenbach, Phys. Rev. E **50**, 5138 (1994).
[16] H. A. Janssen, Z. Ver. Dtsch. Ing. **39**, 1045 (1895).
[17] R. L. Brown and J. C. Richards, *Principles of Powder Mechanics* (Pergamon Press, Oxford, 1970).
[18] R. Nowak, M. Povinelli, H. M. Jaeger, S. R. Nagel, J. B. Knight, and E. Ben-Naim (unpublished).
[19] C. H. Liu, S. R. Nagel, D. A. Schecter, S. N. Coppersmith, S. Majumdar, O. Narayan, and T. A. Witten, Science **269**, 513 (1995).
[20] R. Peralta-Fabi, C. Malaga, and R. Rechtman (private communication).
[21] C. C. Mounfield and S. F. Edwards, Physica A **226**, 12 (1996).
[22] J.-P. Bouchaud, M. E. Cates, and P. Claudin, J. Phys. I **5**, 639 (1995).
[23] E. Clement, C. Eloy, J. Rajchenbach, and J. Duran, *Lectures on Stochastics Dynamics*, Lecture Notes in Physics Vol. XXX (Springer-Verlag, Berlin, 1997).
[24] F. Radjai, M. Jean, J. J. Moreau, and S. Roux, Phys. Rev. Lett. **77**, 274 (1996).
[25] P. G. de Gennes (unpublished).
[26] S. P. Timoshenko and J. N. Goodier, *Theory of Elasticity*, 3rd ed. (McGraw-Hill International Editions, New York, 1987).
[27] J. J. Moreau, Eur. J. Mech. A Solids **13**, 93 (1994).